Statics and dynamics of a polymer chain adsorbed on a surface: Monte Carlo simulation using the bond-fluctuation model

Pik-Yin Lai
Institute of Physics, National Central University, Chung-li, Taiwan 32054, Republic of China
(Received 13 December 1993)

A polymer chain under good solvent condition near a short-range attractive impenetrable wall (xy plane) is investigated by dynamic Monte Carlo simulation using the bond-fluctuation model. For the statics, the adsorption transition is clearly observed and the adsorption transition temperature, T_a for this model is determined. Chain conformation, segment orientation, fraction of segment adsorbed, chain dimensions, and layer thickness as a function of temperature and distance away from the wall are studied and discussed. Our results for the scaling behavior of the radii of gyration and fraction of segment adsorbed confirm previous analytical theories and static simulation results. We also obtain an estimate for the critical exponent which is consistent with previous static simulations of self-avoiding walks. Furthermore, our data on specific heat show another peak, apart from the one at T_a, at a temperature T_2 distinctively below T_a, suggesting a second transition. As for the dynamics, both the time autocorrelation function and the time dependence of the mean square displacement of the center of mass of the chain are studied. We find that the time autocorrelation function in the adsorbed state can be fitted to a stretched exponential form and the relaxation time starts to diverge for temperatures below T_2. The diffusion coefficients for motions parallel (D_z) and perpendicular($D_\perp$) to the z axis are also extracted. D_z shows a sharp drop as the temperature is lowered below the adsorption transition temperature while $D_\perp$ remains constant until around T_2 at which it decreases abruptly. Furthermore we also observe that the lateral diffusion ($D_\perp$) crosses over from a Rouse behavior ($D_\perp \sim N^{-1}$) to a $D_\perp \sim N^{-2}$ behavior for temperatures below T_2. These results are discussed in terms of the appropriate scaling theories.

PACS number(s): 64.70.Pf, 68.35.Rh, 68.45.−v

I. INTRODUCTION

Among the vast field of polymer science, the properties of polymers near a surface or interface is of most current interest, mainly due to the fact that presence of polymeric materials can drastically modify the surface and interfacial properties in a more or less controlled fashion. In particular, the properties of long flexible polymer chains near an impenetrable attractive surface has drawn considerable interests both theoretically [1–17] and experimentally [18–23]. Surface coated with polymers also has important applications in industrial and biological technologies such as stabilization of colloidal suspension, wetting, chromatography, adhesion, biomaterial compatibility, interaction with membranes, etc. The absorption phase transition and the static properties of a *single* polymer chain have been quite well studied [1–7] using field theoretical method and static Monte Carlo simulation [4,5], and various scaling laws and exponents were found near the absorption transition. Exploiting the relation of polymer statistics with the n-vector model of magnetism ($n \to 0$) [24], it has been demonstrated [4] that polymer near an adsorbing surface can be described in an analogous way as the critical behavior of magnets with a free surface. Crossover scaling functions for a single chain near the transition temperature, T_a, have been formulated and verified by static Monte Carlo simulation of self-avoiding walks [4] on diamond lattices. The theoretical understanding is not as detailed as in the case of many chains absorbed near a surface; previous analytic [2,6,9] studies were mainly about the scaling properties of the monomer concentration profile while simulations [10–14] were mostly concerned with the segment distribution of polymer melt confined between two plates. On the other hand, the situation for the dynamical behavior is much less investigated. There has been some study, using molecular dynamics simulation, to probe the microscopic dynamics [15], i.e., local chain segment fast dynamics, of chains near an absorbing wall, but the more interesting information about the slow global dynamics [25] of the entire chain is much less studied. And it is this slow dynamics that is responsible for the macroscopic dynamical properties like diffusion and layer depletion rate, etc. The motion of a polymer chain is considerably slowed down if the chain segments are attracted by a nearby surface. This is a very common phenomenon encountered in surfaces that are coated with polymers. The attraction between the surface and the monomers is essential for the polymers to stay on the surface. How slowly the polymers are moving (due to self-diffusion) depends on the concentration, temperature (surface-monomer interaction energy), and chain lengths. If there are hydrodynamic effects like shear solvent flow, things get more complicated. This problem is of obvious importance in technology and adhesion industry. Analytic theories often involve assumptions and/or approximations and their predictions often cannot be directly tested by the exper-

imental data. At this stage, computer simulations can provide detail and very valuable information both to the analytical picture and the experimental studies.

As a first step to understand the dynamics and structure of adsorbed chains, in this study we perform dynamical Monte Carlo (MC) simulation of a single chain in a good solvent near an adsorbing wall using the bond-fluctuation model. Although the static behavior of the adsorption of a single chain is quite clear, it is still of interest to confirm previous scaling and simulation results using an entirely different model and verify explicitly the universality of the adsorption transition. In addition, contrary to the previous static MC simulations of a single chain [4], our study can probe dynamical quantities such as relaxation times, self-diffusion in the lateral and normal directions, etc. Section II gives some details of the bond-fluctuation model and the simulation method. Section III concerns the results for the static. Results on the dynamical properties are presented in Sec. IV and finally some discussions and outlook are given in Sec. V.

II. THE BOND-FLUCTUATION MODEL AND SOME SIMULATION DETAILS

The bond fluctuation model (BFM) for macromolecular chain [28,29] is used in this simulation. BFM is a lattice model in which each effective monomer occupies a cube of eight sites in a simple cubic lattice. The bond between successive monomers along a chain can be taken from a set of 108 allowed bond vectors obtainable from the set {(2,0,0), (2,1,0), (2,1,1), (2,2,1), (3,0,0), (3,1,0)} by symmetry operations of the cubic lattice. The bond lengths can fluctuate between 2 and $\sqrt{10}$. Self-avoiding interaction between monomers is enforced by the requirement that no two monomers can share a common site. The Monte Carlo procedure starts by choosing a monomer at random and attempt to move it one lattice spacing in one of the six randomly selected directions: $\pm x$, $\pm y$, $\pm z$. This trial move will be accepted if the following three conditions are satisfied: (i) self-avoidance is obeyed, (ii) the new bond vector still belongs to the allowed set, and (iii) the Boltzmann factor $\exp(-\Delta E/k_BT)$ is greater than a random number between 0 and 1, where ΔE is the change in energy due to the trial move, k_B is the Boltzmann constant, and T is the temperature. Henceforth k_B is absorbed in our temperature units. In the course of its motion, no two bonds will ever intersect each other and hence the entanglement effect is taken care of automatically. Because of its more realistic and simple moves, this model is suitable for the study of dynamical properties of polymers.

We consider a polymer chain consisting of N monomers placed inside an $L \times L \times H$ box where one $L \times L$ surface (xy plane) is an adsorbing surface. Periodic boundary conditions are chosen in the x and y directions while the other two boundaries in the z directions are treated as impenetrable walls. To model the adsorption process, we introduce a short range attraction between the monomer and the adsorption wall (the $z = 1$ plane) as follows: there is a negative energy cost $\epsilon < 0$ (which is taken to be -1) if the monomer lies on the adsorbing wall and there is no interaction otherwise apart from self-avoidance. The polymer chain can move anywhere inside the box. In this study, the chain length ranges from $N = 40$ to $N = 100$. As a linear dimension, we use $L = 128$ and $H = 6N + 1$. We verified that near the adsorption regime, H is sufficiently large such that the plane at $z = H$ has no effect on the equilibrium properties of the system. Starting from the high temperature, a polymer chain is allowed to equilibrate for a long time (typically 5 to 10 times of the relaxation time) and statistical averages are then taken for another extended period typically about ten times the relaxation time. The last configuration of the chain is used as the starting configuration for the next run at a lower temperature. In this way, the system is annealed down to low temperatures in which the chain is well adsorbed on the wall. Static and dynamic quantities are measured at different temperatures.

III. STATICS

The static behavior of the adsorption transition of a single polymer chain has been quite well studied analytically [1–4,6]. Making use of the relation of polymer statistics to the correlation function the n-vector model of magnetism in the $n \to 0$ limit [24], it has been demonstrated [4] that polymer near an adsorbing surface can be described in an analogous way as the critical behavior of magnets with a free surface. Exponents describing the power law behavior near the critical transition region and the crossover scaling functions for the radii of gyration and adsorption energy have been obtained [4]. The values of the exponents and the associated scaling functions have been verified by static Monte Carlo simulations of self-avoiding walks [4] on diamond lattices. Here we present our dynamical MC simulation results using bond-fluctuation model on a simple cubic lattice. We obtain the adsorption transition temperature in the BFM which may be relevant to other simulation studies using this model. Furthermore, not only do we confirm previous static simulation results, our result also gives an independent estimate of the critical exponent and hence confirms the universality of the adsorption transition.

A. Chain conformation

We measure the equilibrium properties for various chain lengths and at different temperatures down to $T = 0.1$. The polymer conformation can best be probed directly by snapshot pictures as shown in Fig. 1 for three different temperatures. At high temperature [Fig. 1(a)], no monomer is adsorbed on the surface and the chain behaves more or less the same as a random self-avoiding coil in a good solvent in the bulk. At a lower temperature (below the adsorption temperature T_a), a finite fraction of monomers are adsorbed on the wall while most of the other monomers stay close to the first few layers forming a kind of close packed layer structure in the z direction as shown in Fig. 1(b). As the temperature is further re-

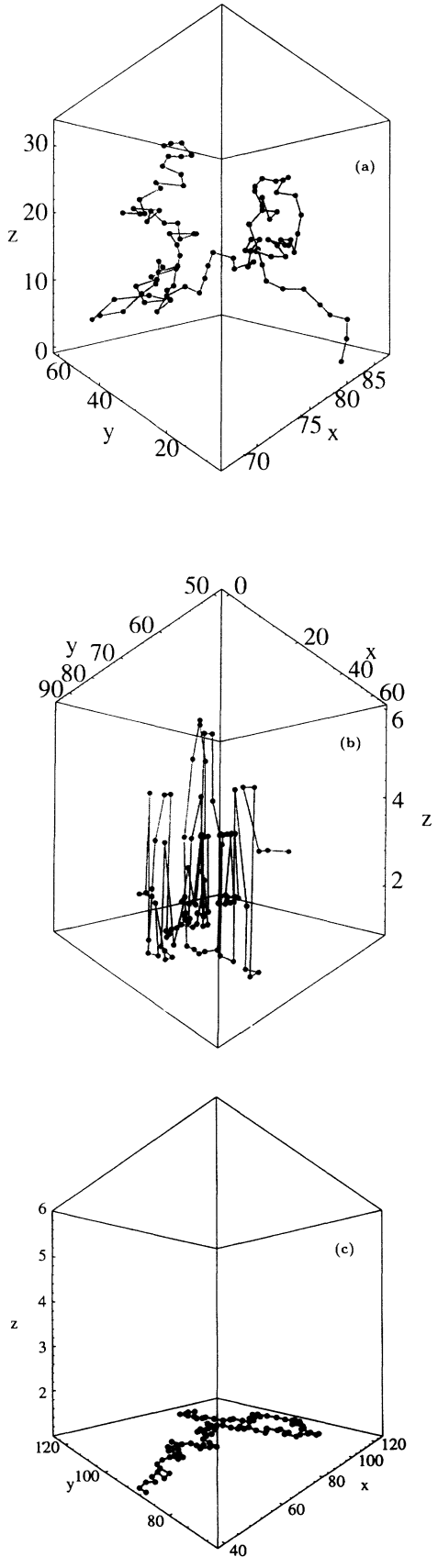

FIG. 1. Snapshots of chain configurations at (a) $T = 1.2$, (b) $T = 0.6$, and (c) $T = 0.1$. Chain length $N = 100$.

duced, the chain lies flat on the adsorbing wall [Fig. 1(c)]. The chain is essentially frozen at this low temperature. To explore the effect of chain dimensions and conformations in a more quantitative manner, we measure the parallel and perpendicular mean square radii of gyration of the chain which are defined as

$$\langle R_{gz}^2 \rangle = \left\langle \frac{1}{N} \sum_{i=1}^{N} (z_i - z_{\text{c.m.}})^2 \right\rangle, \tag{1}$$

$$\langle R_{g\perp}^2 \rangle = \left\langle \frac{1}{N} \sum_{i=1}^{N} \{(x_i - x_{\text{c.m.}})^2 + (y_i - y_{\text{c.m.}})^2\} \right\rangle, \tag{2}$$

$$\langle R_g^2 \rangle = \langle R_{gz}^2 \rangle + \langle R_{g\perp}^2 \rangle, \tag{3}$$

where (x_i, y_i, z_i) are the coordinates of the ith monomer in a chain and $(x_{\text{c.m.}}, y_{\text{c.m.}}, z_{\text{c.m.}})$ is the position of the center of mass of the chain. The angular brackets $\langle\ \rangle$ denote thermodynamic average. Figure 2 shows the radii

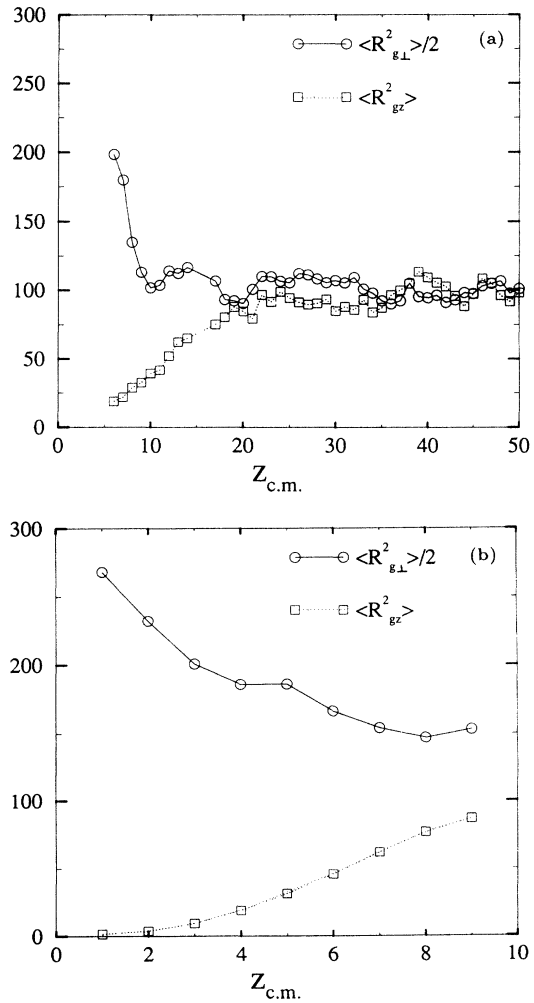

FIG. 2. Radii of gyration as a function of $z_{\text{c.m.}}$ at (a) $T = 1.2$ and (b) $T = 0.7$. Chain length $N = 100$.

of gyration as a function of the z coordinate of the center of mass of the chain at two different temperatures. At high temperature [Fig. 2(a)], when the chain is far away from the wall, the chain is basically isotropic and hence $\langle R_{gz}^2 \rangle \approx \frac{1}{2}\langle R_{g\perp}^2 \rangle$. When the chain is close to the wall, $\langle R_{gz}^2 \rangle$ decreases while $\frac{1}{2}\langle R_{g\perp}^2 \rangle$ increases as compared to its value in the bulk implying the chain deforms to a pancake shape. At this high temperature, the wall is basically neutral as can be confirmed from the fact that the radii of gyration have the same behavior also near the $z = H$ plane (not shown) and the chain can be found in the entire box. This flattening of the chain near an impenetrable wall is purely an entropic effect which has also been observed in other simulation studies [26,27] using different models. Below T_a [$T = 0.7$ in Fig. 2(b)], the chain stays close to the wall for most of the time and no chain is found whose $z_{\text{c.m.}}$ is greater than about a few lattice spacing from the wall.

The orientation of the chain segments can best be monitored by the angle θ between the z axis and the bonds. A convenient quantity to distinguish the directions of the bonds is

$$P_2(\cos\theta) \equiv \frac{1}{2}(3\cos^2\theta - 1). \tag{4}$$

$\langle P_2(\cos\theta) \rangle$ will take values $-\frac{1}{2}$, 0, and 1 for bonds that are perpendicular, randomly oriented, and parallel to z direction. Figure 3 displays the orientation of the ith bond along the chain, θ_i, at various temperatures. At high temperature, the segments are randomly oriented as expected. As the temperature is lowered, $\langle P_2(\cos\theta_i) \rangle$ becomes more negative indicating that the bonds spend more time aligning parallel to the plane of the wall. Notice that near the chain ends, $\langle P_2(\cos\theta_i) \rangle$ is larger, suggesting end segments are freer. At very low temperature ($T = 0.2$) $\langle P_2(\cos\theta_i) \rangle = -\frac{1}{2}$ for all i implying all the segments lie flat on the wall due to the strong adhesion. Another related quantity is the orientation of the chain segment as a function of its position from the wall $\theta(z)$, as shown in Fig. 4. At high temperature, chain segments

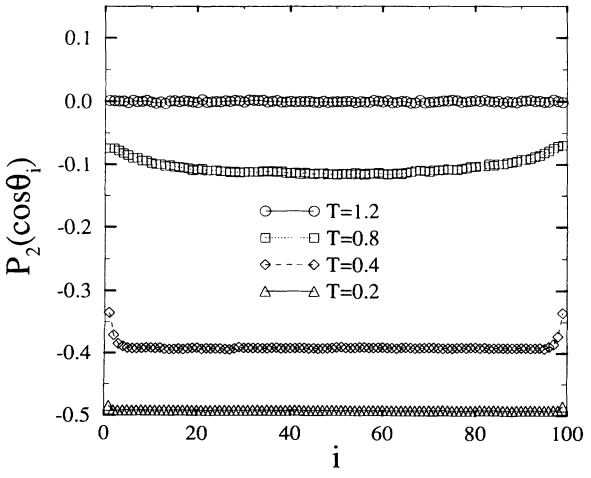

FIG. 3. Average orientation of the ith bond. $\langle P_2(\cos\theta_i) \rangle$ versus i at four different temperatures. $N = 100$.

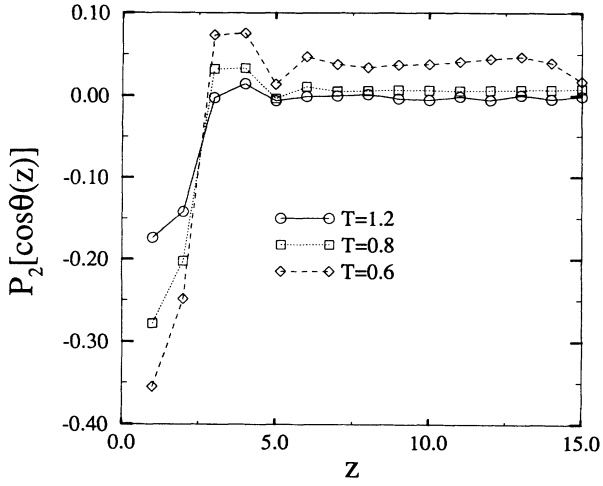

FIG. 4. Average orientation of the bonds as a function of their distance from the wall. $\langle P_2(\cos\theta(z)) \rangle$ versus z at three different temperatures. $N = 100$.

are randomly oriented when they are far away ($z > 5$) from the wall and tend to align parallel to the wall when they are get closer to the wall. As the temperature is lowered, the tendency for the segments close to the wall to lie flat increases. These results are consistent with the picture that the chain assumes a pancake shape when it is close to the wall and the chain will spend more time near the wall when the temperature is lowered.

B. Phase transitions

It has been quite well established [1–6] that the adsorption of a single polymer chain on a short range attractive surface undergoes a critical phase transition. Various scaling laws concerning the radii of gyration and the fraction of adsorbed segments have been formulated [4] and the corresponding exponents obtained by static Monte Carlo simulations [4] on diamond lattices. Here we shall report the static properties near the transition point using dynamical Monte Carlo simulation of the bond-fluctuation model. Following earlier studies [4], we monitor the root-mean-square radii of gyration and the average fraction of monomers adsorbed f_a. In our model, f_a is exactly equal to the average energy per monomer. Figure 5 displays the above quantities as a function of temperature and it clearly shows a sharp transition occurs at $T \simeq 0.9$. Above the transition temperature, no finite portion of the chain is adsorbed and the chain is basically isotropic with $\langle R_{gz}^2 \rangle \simeq \frac{1}{2}\langle R_{g\perp}^2 \rangle$. As the temperature decreases below the transition point, f_a increases and saturates at $f_a \approx 1$ at very low temperature indicating the whole chain lies on the wall. The fact that $\langle R_{gz}^2 \rangle^{1/2}$ decreases while $\frac{1}{2}\langle R_{g\perp}^2 \rangle^{1/2}$ increases as T is lowered is consistent with the fact that the chain gets flattened and attracted towards the wall. However, the overall dimension of the chain ($\langle R_g^2 \rangle^{1/2}$) increases upon reducing temperature below the transition point. At very

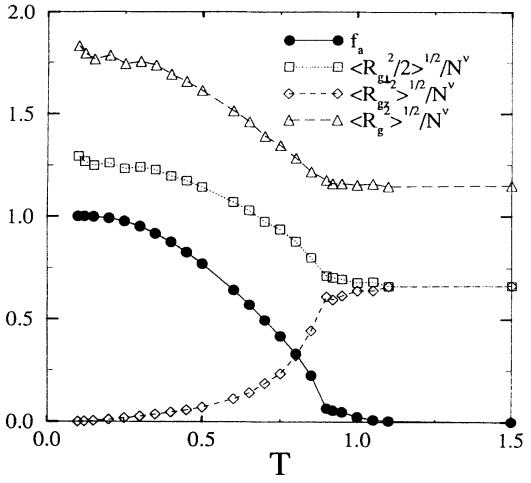

FIG. 5. Scaled radii of gyration, fraction of segment adsorbed as a function of temperature for chain of length $N = 80$. $\nu = 0.588$.

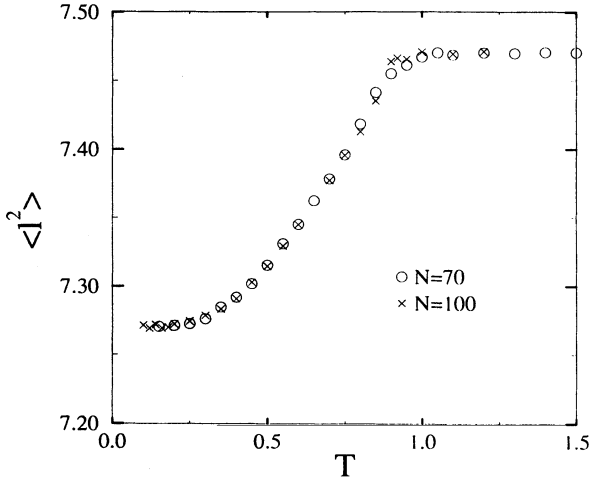

FIG. 7. Mean square bond length between successive monomers $\langle \ell^2 \rangle$ versus T for $N = 70$, 100.

low temperatures ($T < 0.2$), $\langle R_{gz}^2 \rangle^{1/2} \approx 1$ again implying the chain is lying flat on the wall.

For second order phase transitions, fluctuation quantities like the specific heat should diverge near the transition temperature and for finite systems as in our simulation, a peak should appear. The specific heat C as a function of temperature is shown in Fig. 6, the peak around T_a is clearly seen as expected, but in addition to this, another peak appears at a temperature $T_2 \simeq 0.2$ which suggests another phase transition. In fact, the data on $\langle R_g^2 \rangle$ (Fig. 5) also show a kink at T_2 indicating a sharp change in the structure occurs. The transitions at T_a and T_2 can also be revealed from our data on the average bond length $\langle \ell^2 \rangle$. The bond-fluctuation model has the unique feature of variable segment lengths among the lattice polymer models. The mean square bond length often reflects the state of the polymer system. As shown in Fig. 7 $\langle \ell^2 \rangle$ stays almost constant for T above T_a and shows a kink and decreases below the critical point. The fact $\langle \ell^2 \rangle$ decreases while $\langle R_g^2 \rangle^{1/2}$ increases as T is lowered implies that as the chain gets attracted to the wall, it is compressed from an initially isotropic coil to a pancake structure by uncoiling the chain segments. Below T_2, $\langle \ell^2 \rangle$ stays roughly constant upon further cooling; this suggests the polymer chain might be in a "frozen" state. We shall discuss more about this aspect in the section about dynamics.

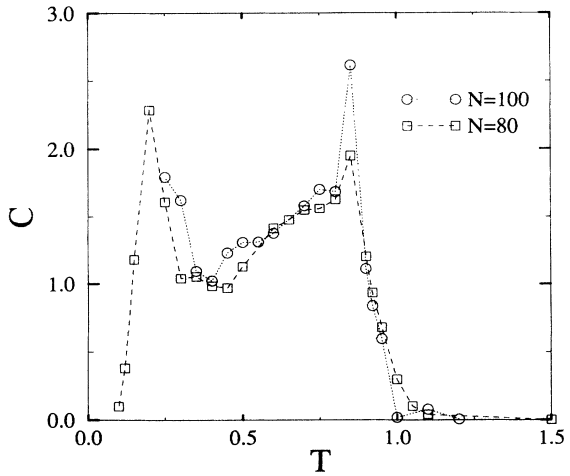

FIG. 6. Specific heat C as a function of temperature T for $N = 80$, 100.

C. Adsorption temperature and critical exponents

The transition temperature T_a of the adsorption transition for the bond-fluctuation model can be obtained by making use of the crossover scaling results by Eisenriegler *et al.* [4],

$$\langle R_{g\perp}^2 \rangle = N^{2\nu} f_\perp(tN^\phi), \tag{5}$$

$$\langle R_{gz}^2 \rangle = N^{2\nu} f_z(tN^\phi), \tag{6}$$

$$f_a = N^{\phi-1} h(tN^\phi), \tag{7}$$

where $t \equiv (T - T_a)/T_a$ and $f_\perp$, f_z, and h are scaling functions. ν is the self-avoiding walk exponent in three dimensions. The value of ν is quite well established from analytical results [30] and simulations [31], we shall take $\nu \simeq 0.588$. To determine T_a for the present model, notice that from Eq. (5), $\langle R_{g\perp}^2 \rangle / N^{2\nu}$ is independent of N at $T = T_a$. Thus a plot of $\langle R_{g\perp}^2 \rangle / N^{2\nu}$ versus T for various chain lengths N will intersect at T_a. Figure 8 shows such a plot and indeed as T increases data for different values of N merge together at some temperature and we obtain $T_a \simeq 0.92 \pm 0.06$. From Eq. (7), $f_a \propto N^{\phi-1}$ at T_a and thus our data can provide an independent estimate for the exponent ϕ. We perform extensive simulations at $T_a = 0.92$ and measure f_a for different chain lengths

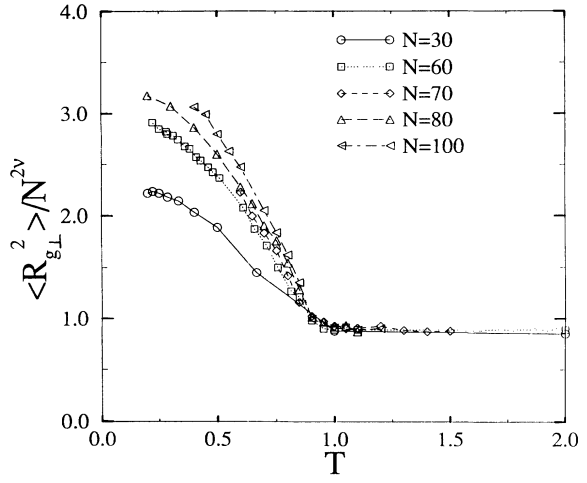

FIG. 8. Scaled radius of gyration $\langle R_{g\perp}^2 \rangle / N^{2\nu}$ versus T for different chain lengths, $\nu = 0.588$.

and the result is shown in Fig. 9. A simple fitting of the data gives $\phi \approx 0.58 \pm 0.15$ which is in agreement with earlier results using static Monte Carlo simulation of self-avoiding walks on diamond lattices ($\phi \simeq 0.58 \pm 0.03$) [4] and simple cubic lattices ($\phi \simeq 0.530 \pm 0.007$) [5]. However, the precision in dynamic Monte Carlo is much lower and our result is unable to resolve the slight discrepancy in the value of ϕ in Refs. [4] and [5]. With $\nu = 0.588$ and $\phi = 0.58$, scaling plots verifying the cross-over scaling laws [Eqs. (5)–(7)] are shown in Fig. 10. The data collapse into a master curve except for some systematic deviations for shorter chain lengths.

The quantity which is relevant to experiments and technological applications is the layer thickness formed by the adsorbed chain. This can be measured by the center of mass position of the chain from the wall $\langle z_{\text{c.m.}} \rangle$ of the adsorbed chain. Figure 11 is a plot of $\langle z_{\text{c.m.}} \rangle$ versus $|t|$ for chains of different lengths in the adsorbed state ($T < T_a$). Our data indicate that the thickness of the adsorbed layer is essentially independent of N for a given temperature and the thickness is roughly proportional to $|t|^{-1}$. This can be understood in terms of the scaling law (6). In the adsorbed state one has $f_z(tN^{\phi}) \sim |t|^{-2\nu/\phi} N^{-2\nu}$ for $|t|N^{\phi} >> 1$ [4] and hence

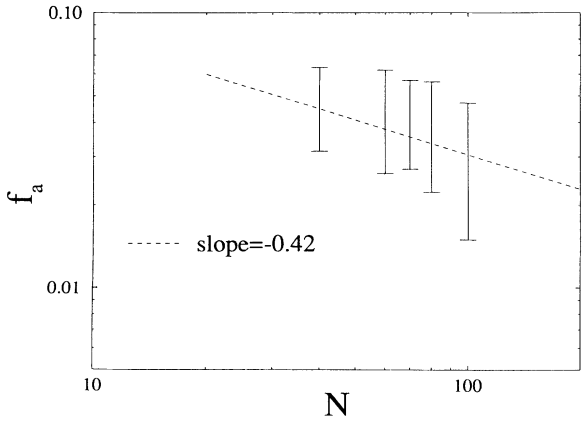

FIG. 9. Log-log plot of f_a versus N at $T_a = 0.92$. Dashed line is a best fit of the data which gives a slope of -0.42.

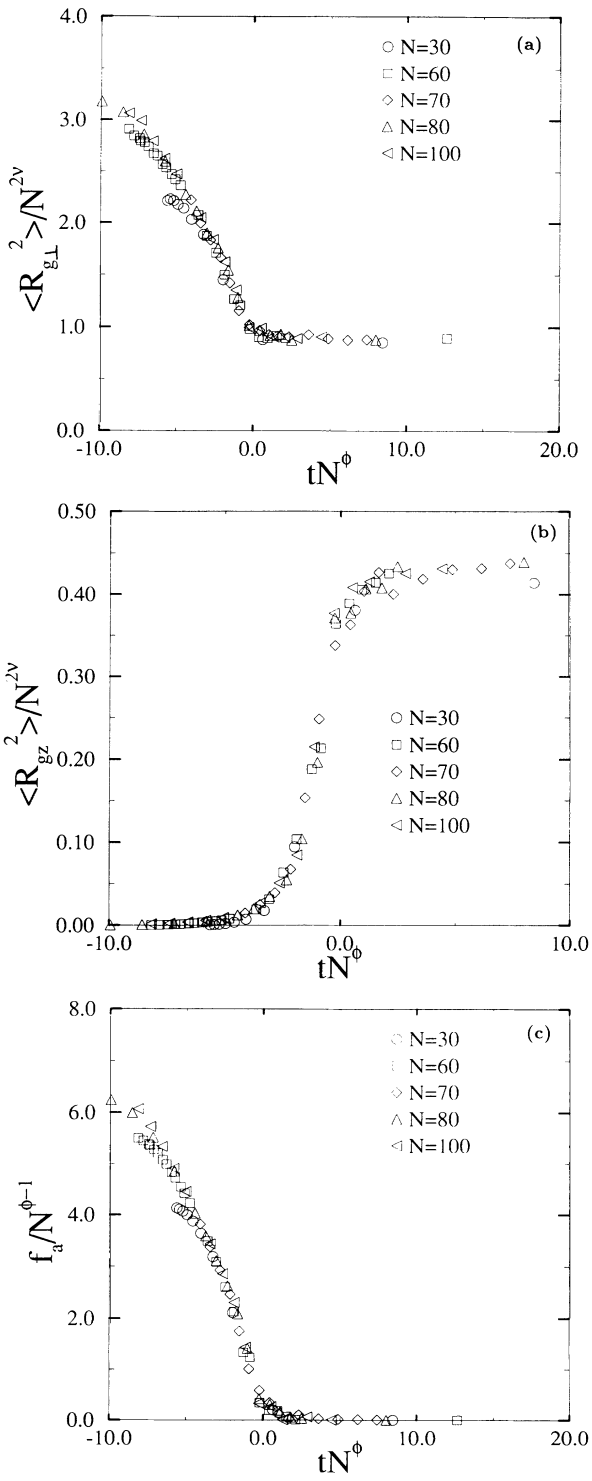

FIG. 10. Scaling plots using $\nu = 0.588$ and $\phi = 0.58$ for different N and temperatures from (a) Eq. (5), (b) Eq. (6), and (c) Eq. (7).

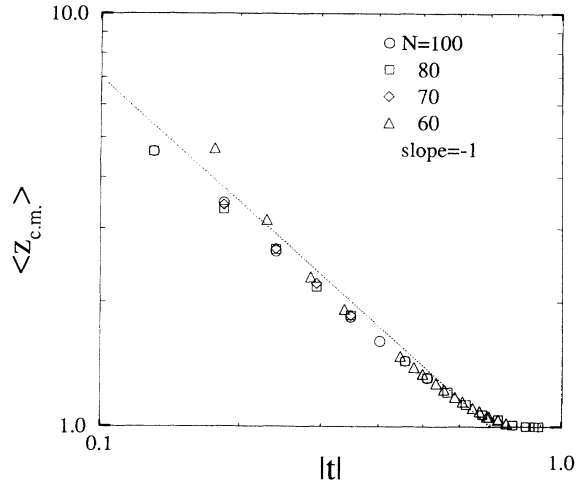

FIG. 11. Log-log plot of $\langle z_{\rm c.m.}\rangle$ versus $|t|$ for chains in the adsorbed states. Dashed line corresponds to a slope of -1.

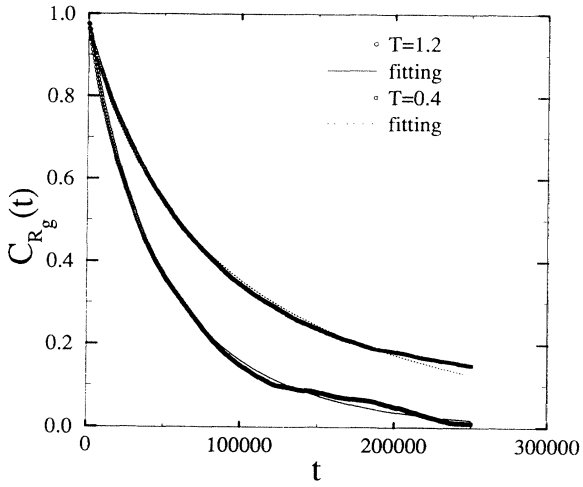

FIG. 12. Time autocorrelation function for the radius of gyration as defined in Eq. (9) at $T = 1.2$ and $T = 0.4$ for $N = 100$. t is in units of MCS/momoner. Solid and dashed lines are the two parameter fits from Eq. (10) for data at $T = 1.2$ and 0.4, respectively.

$$\langle z_{\rm c.m.}\rangle \propto \langle R_{gz}^2\rangle^{1/2} \propto |t|^{\nu/\phi} \tag{8}$$

and $\nu/\phi = 0.588/0.58 \approx 1$.

IV. DYNAMICS

Dynamic phenomena in adsorbed polymer are much less understood. They are clearly of interest in understanding the dynamical response to such a layer under external perturbations. To contribute towards a basic understanding of the dynamical properties, we have obtained information on the time autocorrelation function, time dependence of mean square displacement of monomers and the diffusion coefficients. Time is measured in units of Monte Carlo steps per monomer (MCS/monomer), one MCS/monomer means that on average every monomer has attempted to move once. Here we will use the symbol t for time; this should not be confused with the reduced temperature in preceding sections.

A. Time autocorrelation function, relaxation time, and glassy behavior

We measure the time autocorrelation function for the radii of gyration R_g, R_{gz}, and $R_{g\perp}$; since the correlation function of R_g decays the slowest, we will concentrate on it. Figure 12 shows the time autocorrelation function $C(t)$ for the radius of gyration R_g, defined as

$$C(t) \equiv \frac{\langle (R_g(t) - \langle R_g\rangle)(R_g(0) - \langle R_g\rangle)\rangle}{\langle R_g^2\rangle - \langle R_g\rangle^2} \tag{9}$$

at high and low temperatures. $C(t)$ decays much slower as T decreases. At temperatures above T_a, $C(t)$ can be roughly fitted to an exponential decay, but at low temperatures $C(t)$ decays considerably slower than a simple exponential decay. Instead $C(t)$ can be fitted to a stretched exponential of the form

$$C(t) = \exp\left(-(t/\tilde{\tau})^{\alpha}\right), \tag{10}$$

where $\tilde{\tau}$ and α are fitting parameters. The quality of the fittings are quite good with a χ^2 of the order 10^{-2}. We found that $\alpha \approx 1$ for temperatures above T_a and for $T < T_a$, $\alpha < 1$ and keeps decreasing as T is lowered. Also shown in Fig. 12 are the fitted functions, $\alpha \simeq 0.96$ for $T = 1.2$ and $\alpha \simeq 0.75$ for $T = 0.4$. At very low temperatures (~ 0.2), $C(t)$ decays very slowly but a stretched exponential form can still be fitted. The relaxation time, τ, can be calculated from the integral of $C(t)$. Assuming $C(t)$ is of the stretched exponential form in (10), one gets

$$\tau = \int_0^{\infty} C(t)dt = \frac{\tilde{\tau}}{\alpha}\Gamma\left(\frac{1}{\alpha}\right). \tag{11}$$

Figure 13 shows the variation of τ as a function of T for different chain lengths. τ remains roughly constant for temperatures above T_a and starts to rise slowly for $T < T_a$. Around the same low temperature at which a peak appears in the specific heat, $T_2 \approx 0.2$, τ increases drastically as temperature is further lowered. The apparent divergence of τ at very low temperature is often related to some "glassy" behavior suggesting the chain is basically frozen on the wall. A speculative suggestion for a glass transition of adsorbed chains has also been made by Kremer [32]. We attempt to fit the low temperature relaxation time with the Vogel-Fulcher law [33] that describes glass transitions:

$$\tau = \tau_{\infty} \exp\left(\frac{A}{T - T_{\rm VF}}\right), \tag{12}$$

where τ_{∞} is the high temperature relaxation time, $T_{\rm VF}$ is Vogel-Fulcher temperature, and A is some parameter

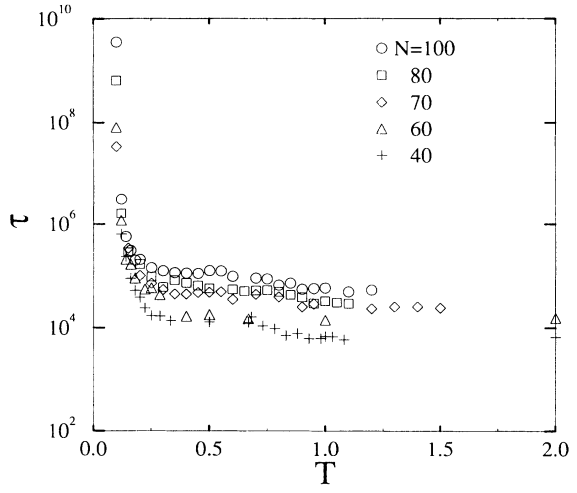

FIG. 13. The relaxation time τ in units of MCS/monomer versus T as defined in Eq. (11) for chains of various lengths.

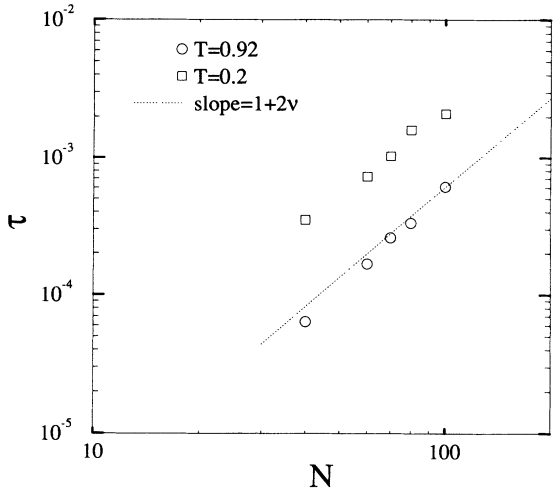

FIG. 15. Log-log plot of τ versus N at $T = 0.92$ and $T = 0.2$. Uncertainties in τ are about the size of the symbols. Dotted line corresponds to a slope of $1 + 2\nu = 2.176$.

which may be interpreted as a measure of the activation energy. Figure 14 shows a plot of $1/\ln(\tau/\tau_\infty)$ versus T for $N = 100$. The data fall on a straight line for $T < T_2$ consistent with the Vogel-Fulcher behavior, with $T_{VF} \simeq 0.09$ and $A \simeq 0.12$. It should be noted that a recent molecular dynamic study on oligomer films [16] also indicated a glassy behavior on strongly absorbed surfaces.

The dependence of the relaxation time on chain length N is also studied. At high temperatures in which the effect of the attractive wall can be neglected, we expect the chain should follow Rouse dynamics [25,34,35] with the relaxation time scales as

$$\tau \sim N^{1+2\nu}. \tag{13}$$

This is indeed observed at high temperatures even up to T_a. Figure 15 is a plot of τ versus N at $T = 0.92$ and 0.2; the data at $T = T_a$ obey quite nicely the Rouse dynamics (13). The relaxation times at $T = 0.2$ are longer, but surprisingly the data still seem to be consistent with the Rouse dynamics. This will be further discussed in the next section.

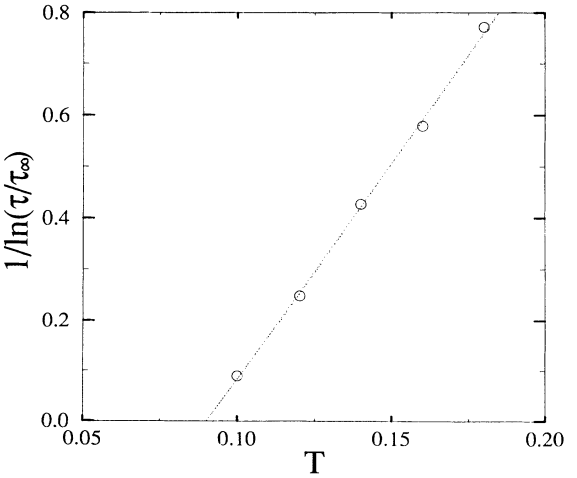

FIG. 14. $1/\ln(\tau/\tau_\infty)$ versus T for low temperature data ($T < 0.2$). Chain length $N = 100$.

B. Mean-square displacements and diffusion constants

To probe the dynamical behavior of the chain, we measure the time dependences of the mean-square displacements of the center of mass of the chain in the direction parallel to and perpendicular to z axis,

$$g^z_{\text{c.m.}}(t) = \langle (z_{\text{c.m.}}(t) - z_{\text{c.m.}}(0))^2 \rangle, \tag{14}$$

$$g^\perp_{\text{c.m.}}(t) = \langle (x_{\text{c.m.}}(t) - x_{\text{c.m.}}(0))^2 + (y_{\text{c.m.}}(t) - y_{\text{c.m.}}(0))^2 \rangle. \tag{15}$$

$g^z_{\text{c.m.}}(t)$ [Fig. 16(a)] and $\frac{1}{2} g^\perp_{\text{c.m.}}(t)$ [Fig. 16(b)] and at different temperatures are displayed. At high temperature, $g^z_{\text{c.m.}}(t)$ and $g^\perp_{\text{c.m.}}(t)/2$ are almost identical as expected, furthermore both of them scale as $\sim t$ indicating free diffusions in both directions. $g^z_{\text{c.m.}}(t)$ decreases with T for $T < T_a$ implying the chain is being trapped by the attractive wall and is unable to diffuse away from it. On the other hand, as T decreases $g^\perp_{\text{c.m.}}(t)$ remains more or less unaffected (with a very small decrease) for temperatures down to $T \simeq T_2$. Upon further lowering the temperature, $g^\perp_{\text{c.m.}}(t) \sim t$ holds only for early times, at intermediate times ($5000 < t < 100\,000$), one can see a motion much slower than free diffusion, and at larger times the $\sim t$ behavior is recovered.

From the analysis of the center of mass motion of the chain in directions parallel to and perpendicular to the z axis, we can obtain the diffusion constants in these two directions, defined as

$$D_z = \lim_{t\to\infty} \frac{1}{2t} g^z_{\text{c.m.}}(t), \tag{16}$$

$$D_\perp = \lim_{t\to\infty} \frac{1}{4t} g^\perp_{\text{c.m.}}(t). \quad (17)$$

The apparent diffusion coefficient decreases systematically with t and high precision data are required to carry out the extrapolation to $t \to \infty$ in Eqs. (16) and (17). The resulting data for D_z and $D_\perp$ as a function of T are shown in Fig. 17. $D_z \simeq D_\perp$ at high temperatures as expected. As T is lowered D_z decreases abruptly at $T \simeq T_a$ and quickly drops to almost zero while $D_\perp$ remains essentially constant for temperatures down to about T_2. For temperatures below T_2, $D_\perp$ starts to fall quite sharply to small values. As in the data for the relaxation time, there appears to be two temperatures at which the dynamics of the system changes drastically. The first being the transition temperature T_a, the second is at a lower temperature around $T_2 \simeq 0.2$ below which the chain appears to be in a kind of glassy or frozen state. We expect at high temperatures, the dynamics for the single chain should obey the Rouse model with $D \sim N^{-1}$. This is indeed observed for both D_z and $D_\perp$ at high temperature. Even down to T_2, our data for $D_\perp$ is still consistent with the Rouse behavior (Fig. 18). However, D_z shows a strong deviation from the Rouse behavior for T close to and below T_a; furthermore the variation of D_z cannot be described by a power law behavior at T_a. The behavior of $D_\perp$ in the fully adsorbed state is also shown in Fig. 18 ($T = 0.1$), it is consistent with the power law $D_\perp \sim N^{-2}$. A crossover from the Rouse behavior ($\sim N^{-1}$) to a $\sim N^{-2}$ behavior is observed for the lateral diffusion as T decreases from T_2 to even lower temperatures. It should be noted that a similar behavior, with the mobility being proportional to N^{-2}, has been suggested [17] in diffusive adsorbed layers by assuming a self-similar concentration profile.

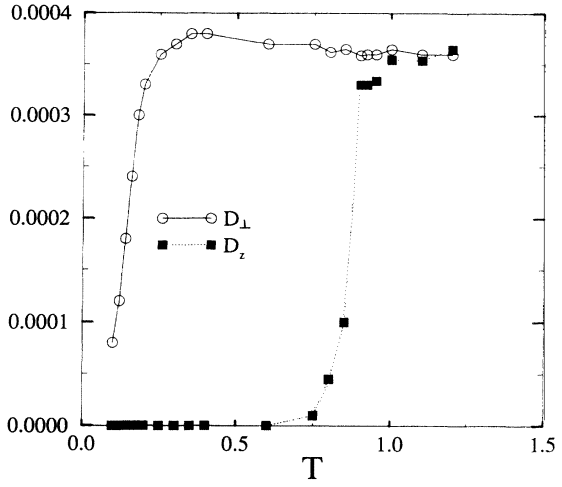

FIG. 17. Diffusion coefficients parallel and perpendicular to the z axis, D_z and $D_\perp$, in units of (MCS/monomer)$^{-1}$, as a function of T for chain of length $N = 100$.

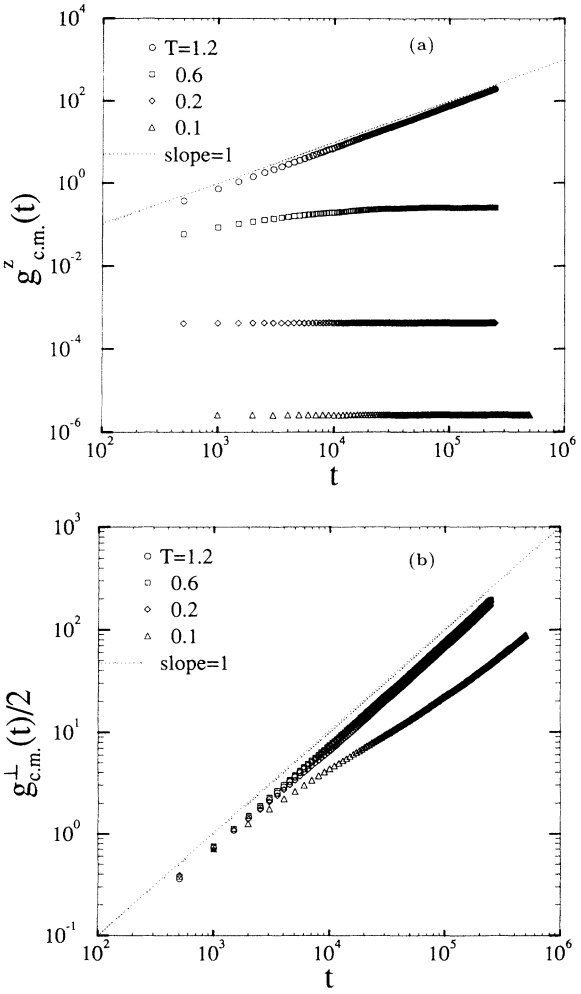

FIG. 16. Mean square displacements (a) $g^z_{\text{c.m.}}(t)$ and (b) $\frac{1}{2}g^\perp_{\text{c.m.}}(t)$ at various temperatures for chain of length $N = 100$ shown in a log-log plot. Dashed line denotes a slope of 1.

V. DISCUSSIONS AND OUTLOOK

In this paper, the bond-fluctuation model is used to simulate the static and dynamic behavior of adsorption

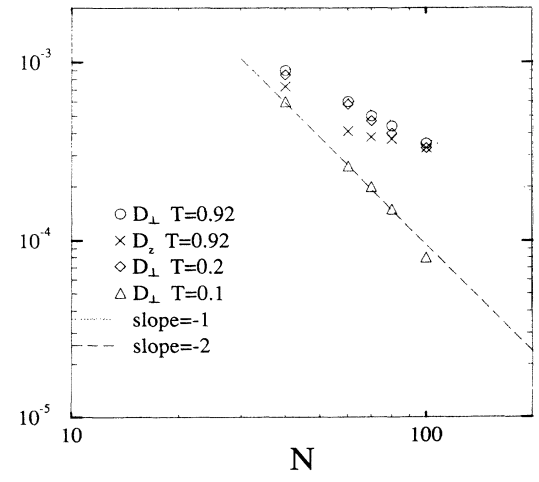

FIG. 18. Log-log plot of D_z and $D_\perp$ versus N at $T_a = 0.92$, $T = 0.2$ and 0.1. Dotted and dashed lines denote a slope of -1 and -2, respectively.

of a polymer chain near an attractive wall. Varying the chain length N and the temperature T over a wide range, we verified the predictions from analytical theories for the static adsorption transition. In particular we obtained an estimate for the exponent ϕ which is in agreement with both previous MC simulations using static method on different lattices [4,5]; unfortunately the precision in dynamical simulations is not sufficient to settle the slight discrepancy between previous results. More interestingly, at T_2 which is much lower than T_a, we observed a structural change as revealed in the peak in specific heat (Fig. 6), the data on $\langle R_g^2 \rangle$ (Fig. 5), and the average bond length (Fig. 7); this should be related to the glassy behavior as observed in the dynamics.

For the dynamics, we found that the relaxation of the chain is very slow at low temperatures with the time autocorrelation function described by a stretched exponential. Furthermore, at very low temperature $T < T_2$, the system shows a glassy behavior with the relaxation time increasing drastically, which can be described by the Volgel-Fulcher law. These results suggest that at this very low temperature the chain is almost entirely stuck to the wall and is trapped in some glassy state; it has to overcome a huge activation energy barrier in order to relax to another state. This slow relaxation may be due to the fact that when the monomers are first adsorbed onto the surface, the chain is probably not in its equilibrated configuration in the adsorbed state and the chain has to rearrange almost all of its monomers at the same time to relax and this could cause a huge activation barrier. The aging effect [23] observed in a recent experiment on the kinetics of chain adsorption also indicated a very slow rearrangement of adsorbed chains towards conformational equilibrium; this may share the same origin of the slow dynamics in our results. The sharp drop of the diffusion constant D_z at T_a which implies the chain being localized by the attractive wall is somewhat expected. On the other hand, the abrupt decrease of $D_\perp$ around T_2 is more interesting; it reflects the chain is in a glassy state. Figure 18 indicates that $D_\perp$ crosses over from the Rouse behavior ($\sim 1/N$) to a $\sim N^{-2}$ behavior at very low temperature ($< T_2$), suggesting that the lateral diffusion in the fully adsorbed state ($f_a = 1$ at this temperature) is still very much different from a genuine two-dimensional system where strictly Rouse behavior was found [29]. A N^{-2} behavior for lateral diffusion suggested for dense adsorbed layers by assuming some sort of reptation mechanism in a self-similar concentration profile [17] may have some relation to our result, but the connection is not obvious.

We observed the expected Rouse behavior for the relaxation time [Eq. (13)] at high temperatures, but the apparent consistency with the Rouse behavior even at low temperatures ($T = 0.2$, Fig. 18) is somewhat surprising. This behavior may be understood as follows: the time needed for the polymer to diffuse a distance of the order of the radius of gyration should be proportional to the relaxation time, and thus $\tau \sim \langle R_g^2 \rangle / D$. At low temperatures ($T_a < T < T_2$), $D = D_z + D_\perp \simeq D_\perp$, and

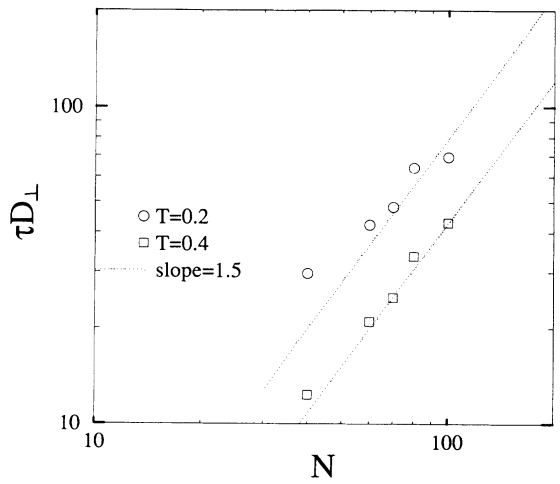

FIG. 19. Log-log plot of $\tau D_\perp$ versus N at $T = 0.4$ and 0.2. Dashed lines denote a slope of 1.5.

using the scaling laws (5), (6), one has $\tau \sim [f_\perp(tN^\phi) + f_z(tN^\phi)]N^{2\nu}/D_\perp$. From the asymptotic behavior [4] of $f_\perp(x) \sim x^{2(\nu_{2d}-\nu)/\phi}$ and $f_z \sim x^{-2\nu/\phi}$ for $|x| << 1$ where $\nu_{2d} = 3/4$ is the self-avoiding walk exponent in two dimensions, one arrives at

$$\tau D_\perp \approx aN^{2\nu_{2d}} + b \tag{18}$$

for some constants a and b. Since $D_\perp \sim N^{-1}$ still holds for $T > T_2$, one has $\tau \approx aN^{2.5} + bN$ and a naive fitting of τ as a power in N will give an effective exponent close to $1 + 2\nu \simeq 2.18$ and thus an apparent agreement with the Rouse behavior. To check this, we plot in Fig. 19 $\tau D_\perp$ versus N in a log-log plot; one expects a straight line with a slope of $2\nu_{2d} = 1.5$ results for large values of N from (18). This is indeed the case.

Our results on both statics and dynamics revealed that apart from the already known adsorption transition at T_a, there exists another transition at T_2, possibly dynamical in origin, and the system transforms to a glassy state. We hope that our work will stimulate more detailed analytical work, especially for the dynamics, to explain those features of our results where no detailed theoretical explanation has yet existed. Also experiments probing direct information on the dynamics of the chains would be also very valuable. In future studies, we plan to investigate the kinetics of adsorption and the effect of shear flow; the structure and dynamics of adsorbed layer formed many chains that are currently under investigation.

ACKNOWLEDGMENTS

We thank National Council of Science of Taiwan under Grant No. NSC 83-0208-M-008-036 for support. Computing time partially supported under Grant No. NSC 82-0208-M-008-094 is gratefully acknowledged.

[1] E. Eisenriegler, *Polymers Near Surfaces* (World Scientific, Singapore, 1993).
[2] P. G. de Gennes, Macromolecules **14**, 1637 (1981).
[3] J. M. Hammersley, G. M. Torrie, and S. G. Whittington, J. Phys. A **15**, 539 (1982).
[4] E. Eisenriegler, K. Kremer, and K. Binder, J. Chem. Phys. **77**, 6296 (1982).
[5] H. Meirovitch and S. Livne, J. Chem. Phys. **88**, 4507 (1988).
[6] P. G. de Gennes and P. Pincus, J. Phys. Lett. (Paris) **44**, L241 (1983).
[7] K. De'Bell and T. Lookman, Rev. Mod. Phys. **65**, 87 (1993).
[8] J. M. H. M. Scheutjens and G. Fleer, J. Chem. Phys. **83**, 1619 (1979); **84**, 178 (1980); Macromolecules **18**, 1882 (1985).
[9] E. Eisenriegler, J. Chem. Phys. **79**, 1052 (1983).
[10] I. A. Bitsanis and G. ten Brinke, J. Chem. Phys. **99**, 3100 (1993).
[11] G. ten Brinke, D. Ausserre, and G. Hadziioannou, J. Chem. Phys. **89**, 4347 (1988).
[12] S. K. Kumar, M. Vacatello, and D. Y. Yoon, J. Chem. Phys. **89**, 5206 (1988); Macromolecules **23**, 2189 (1990).
[13] W. G. Madden, J. Chem. Phys. **87**, 1405 (1987).
[14] D. N. Theodorou, Macromolecules **21**, 1400 (1988).
[15] I. A. Bitsanis and G. Hadziioannou, J. Chem. Phys. **92**, 3827 (1990).
[16] I. A. Bitsanis and C. Pan, J. Chem. Phys. **99**, 5520 (1993).
[17] P. G. de Gennes, C. R. Acad. Sci. Paris II **306**, 183 (1988).
[18] J. N. Israelachvili and S. J. Kott, J. Chem. Phys. **88**, 7162 (1988).
[19] J. P. Montfort and G. Hadziioannou, J. Chem. Phys. **88**, 7187 (1988).
[20] P. F. Luckham and J. Klein, J. Chem. Soc. Faraday Trans. **86**, 1363 (1990).
[21] L. Auvray, P. Auroy, and M. Cruz, J. Phys. (France) I **2**, 942 (1992).
[22] L. Auvray, M. Cruz, and P. Auroy, J. Phys. (France) II **2**, 1133 (1992).
[23] P. Frantz and S. Granick, Phys. Rev. Lett. **66**, 899 (1991).
[24] P. G. de Gennes, J. Phys. Lett. (Paris) **36**, L55 (1979).
[25] M. Doi and S. Edwards, *The Theory of Polymer Dynamics* (Oxford University Press, Oxford, 1986).
[26] M. R. Wattenbarger, H. S. Chan, D. F. Evans, V. A. Bloomfield, and K. Dill, J. Chem. Phys. **93**, 8343 (1990).
[27] J. S. Wang and K. Binder, Makromeol. Chem. Theory Simulation **1**, 20 (1992).
[28] I. Carmesin and K. Kremer, Macromolecules **21**, 2819 (1988).
[29] I. Carmesin and K. Kremer, J. Phys. (Paris) **51**, 915 (1990).
[30] J. C. Le Guillou and J. Zinn-Justin, Phys. Rev. Lett. **39**, 95 (1977); Phys. Rev. B **21**, 3976 (1980).
[31] K. Kremer, A. Baumgärdner, and K. Binder, Z. Phys. **40**, 331 (1981).
[32] K. Kremer, J. Phys. (Paris) **47**, 1269 (1986).
[33] H. Vogel, Phys. Z **22**, 645 (1921); G. S. Fulcher, J. Am. Ceram. Soc. **8**, 339 (1925).
[34] P. E. Rouse, J. Chem. Phys. **21**, 1272 (1952).
[35] P. G. de Gennes, *Scaling Concepts in Polymer Physics* (Cornell, Ithaca, 1979).